



Contents lists available at ScienceDirect



Catalysis Today

journal homepage: www.elsevier.com/locate/cattod

Mesoporous niobiosilicate NbMCF modified with alkali metals in the synthesis of chromene derivatives

Agata Smuszkiewicz^a, Jesús Lopez-Sanz^{a,b}, Izabela Sobczak^{b,**}, Maria Ziolek^b, Rosa M. Martín-Aranda^a, Elena Soriano^{c,***}, Elena Pérez-Mayoral^{a,*}

^a Departamento de Química Inorgánica y Química Técnica, Universidad Nacional de Educación a Distancia, UNED, Paseo Senda del Rey 9, E-28040 Madrid, Spain

^b Adam Mickiewicz University, Faculty of Chemistry, Umultowska 89b, 61-614 Poznań, Poland

^c Instituto de Química Orgánica General (CSIC), C/ Juan de la Cierva 3, E-28006 Madrid, Spain

ARTICLE INFO

Article history:

Received 30 July 2015

Received in revised form 11 February 2016

Accepted 19 February 2016

Available online xxx

Keywords:

Heterogeneous catalysis

Niobium Mesoporous Cellular Foams

Heterocyclic ring systems

Theoretical calculations

ABSTRACT

We report the synthesis, characterization and activity of new series of catalysts based on Niobium Mesoporous Cellular Foams (NbMCF), modified with alkaline metal elements. These materials exhibit very different acid-base properties attributed to the Nb source for the preparation of the catalysts and the presence and loading of different alkaline metals.

The Me/NbMCF materials (where Me are alkaline metals) were tested in the reaction of 2-hydroxybenzaldehyde and ethyl cyanoacetate, under solvent-free conditions, at room temperature, leading to mixtures of the corresponding chromenes **4** and **5**, as mixtures of diastereomers *erythro/threo*, in a 2:1 ratio, respectively, with good to excellent yields.

Our experimental results indicate that the metal loading on the catalysts and the acid-base character, and the texture parameters are probably determining factors in the reactivity and the observed diastereoselectivity.

The computational study suggests that the presence of alkaline oxides on Me/NbMCF catalyst, exhibiting strong basicity, activates the formation of the nucleophile species, the corresponding enolate, and initiates the reaction. However, the cation size has a deep impact on the stability of the reactant complex so that the effective aldolization could be obstructed by the presence of the bulkier centers.

© 2016 Elsevier B.V. All rights reserved.

1. Introduction

Since the discovery of the mesoporous silica MCM-41 by Mobil Corporation in 1992 [1] the interest and investigation concerning these materials have been growing and a huge number of new materials, with different chemical composition, structure and novel pore geometry, have been reported [2,3]. The large surface areas and pore size, periodical structure, the possibility of modification of their silica walls, biocompatibility and biodegradability are the most relevant properties of mesoporous silicas making them interesting materials with application in different research areas [4]. This type of silicas has been extensively studied in adsorption and separation of gases. Particularly, MCM-41 [5], SBA-15 [6] and MCF

[7], all of them modified with amine groups, have been reported as efficient adsorbents of CO₂. Besides, MCM-48 and SBA-15 found their application as adsorbents of heavy metals. In other sense, metallosilicates such as Al-SBA-15 [8] and Pt/SBA-15 [9] have been applied as adsorbents of volatile organic compounds (VOCs).

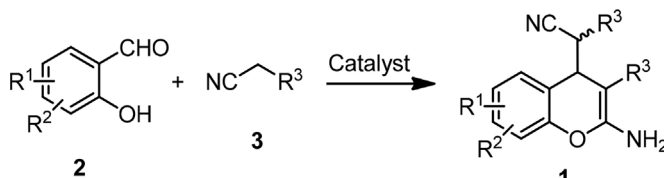
Furthermore, mesoporous silicas have been extensively used in catalysis. In this context, our research group possesses a wide experience in this field, applying mesoporous silicas as heterogeneous catalysts in the synthesis of heterocyclic compounds with biological properties [10]. In particular, we have recently reported novel series of mesoporous silicas with different acid-base properties in the synthesis of quinolones and quinolines, via Friedlander reaction, the synthesis of coumarins through Knoevenagel condensation and the N-alkylation of pyrazole, all of these transformations catalyzed by amino grafted MCM-41 and SBA-15-based materials. We also reported the isomerization of olefins, especially Eugenol and Safrole, catalyzed by amino-grafted metallosilicates. More recently, we reported an experimental and theoretical study concerning the catalytic behavior and of amino-grafted NbMCF in the

* Corresponding author.

** Corresponding author.

*** Corresponding author.

E-mail address: eperez@ccia.uned.es (E. Pérez-Mayoral).



Scheme 1. Synthesis of chromenes **1** from 2-hydroxybenzaldehydes **2** and nitriles substituted at α position **3**.

synthesis of nitrogen heterocycles also through the Friedländer reaction [11].

Mesoporous Cellular Foams (MCF) are a relatively new class of silica materials, easy to be modified, with a cell size between 24 and 42 nm interconnected by window of size between 9 and 22 nm, exhibiting very high surface area and porosity [12]. As other mesoporous silicas, their properties can be changed by incorporation of metals within the framework. In this sense, this type of mesoporous silicas has been reported by some of us in the production of biofuels additives [13], esterification reactions with glycerol [14], and also for the selective oxidation of methanol to formaldehyde [15].

The goal of this paper is the development of a new environmental friendly methodology for the efficient synthesis of 2-amino-4H-chromenes by using NbMCF materials as catalytic agents. 4H-Chromene derivatives are six-membered oxygen heterocycles widely distributed in nature [16] and synthetic drugs, with relevant biological properties [17]. One of the simplest synthetic approaches for the preparation of 2-amino-4H-chromenes **1** is the reaction between 2-hydroxybenzaldehydes **2** and nitriles substituted at α position **3** (Scheme 1). However, only a few examples of heterogeneous catalysts for this transformation have been reported. Thus, Amberlyst A-21 [18], tin(IV) oxide doped hydroxalcites [19], molecular sieves and Al₂O₃ [20] have been reported as catalysts for the synthesis of 4H-chromenes **1** with goods yields although during prolonged reaction times or in the presence of solvents.

In continuation with our studies, we report herein the investigation of the catalytic behavior of novel series of NbMCF materials, prepared from two different Nb sources and modified with alkaline metals, in the synthesis of 4H-chromene derivatives (**1**), through multicomponent reactions (MCRs), between substituted 2-hydroxybenzaldehydes (**2**) and ethyl cyanoacetate (**3**), under solvent-free and mild conditions. Our aim also is to understand the reaction mechanism and the influence of basic character of the MCF materials on the reaction.

2. Materials and methods

2.1. Synthesis of MCF and NbMCF materials

2.1.1. MCM material

MCF was prepared by one-pot synthesis method described in Ref. [21]. First, Pluronic 123 (PL—poly(ethylene glycol)-block-poly(propylene glycol)-block-poly(ethylene glycol)-block) (8 g, 1.4 mmol) was dissolved in 300 g of 0.7 M HCl solution at 308–313 K. Next, 1,3,5trimethylbenzene (TMB) (12 g, 99.84 mmol) (TMB/PL = 1.5) and NH₄F (0.0934 g, 2.52 mmol) were added under vigorous stirring. Following 2 h of stirring, TEOS (17.054 g, 81.99 mmol) was added. The final mixture was stirred at 308–313 K for 24 h and then transferred into a polypropylene bottle and heated at 373 K under static conditions for 24 h. The solid product was recovered by filtration, washed with distilled water and dried at room temperature. The template was removed from the as synthesized material by calcination at 773 K for 8 h under static conditions.

2.1.2. NbMCF materials

For the preparation of NbMCF materials, the synthesis procedure was modified in order to introduce niobium. Two kinds of niobium-containing materials were prepared: NbMCF(ox) and NbMCF(Et), depending on the metal source. In the NbMCF(ox) synthesis ammonium niobate(V) oxalate hydrate (C₄H₄NNbO₉) was added to the gel containing Si source while keeping the TEOS/Nb molar ratio = 64 constant. The source of Nb was added to the mixture 10 min after TEOS admission.

The preparation of NbMCF(Et) material followed the procedure described above, but TMB/PL ratio = 0.75 was applied (8 g, 1.4 mmol of Pluronic and 6 g, 49.92 mmol of TMB). Niobium ethoxide was used as a source of niobium (Si/Nb molar ratio = 64 as assumed).

In order to establish niobium content in NbMCF, XRF technique was applied.

2.2. Modification of NbMCF materials with alkali metals

NbMCF supports were impregnated by using the incipient wetness method with aqueous solution of MeCH₃COO (Me = Li, Na, K, Rb, Cs). The outgassed NbMCF(ox) and NbMCF(Et) (after treatment at 373 K for 3 h in the oven and 1 h at 373 K in an evaporator flask) were filled in with the appropriate amount of an aqueous solution of alkali metal acetate (CH₃COOLi, CH₃COONa, CH₃COOK, CH₃COORb or CH₃COOCs, a volume of the solution was a little bit higher than the pore volume of the support) and rotated and heated in an evaporator flask at 373 K. The impregnated powder was dried at 373 K for 18 h and then calcined at 723 K for 10 h in the oven. Two series of catalysts were obtained: Me/NbMCF(ox) and Me/NbMCF(Et), where Me = alkali metal.

The amount of alkali metal acetate used for the impregnation was calculated for the loading of metal equal to 0.5 mmol per 1 g of NbMCF support. Such value gives rise to the following weight percent of metals: Li—0.35%; Na—1.15%; K—1.96%; Rb—4.27; Cs—6.65% Rb-4.27%. The surface area of the modified materials differs from that of the parent one and therefore the mole number of alkali metal cations calculated per m²g⁻¹ of the supports was calculated and shown in Table 1.

2.3. Characterization

The materials prepared were characterized using XRF, N₂ adsorption/desorption, UV-vis and test reactions.

X-ray fluorescence (XRF) was applied using MiniPal-Philips. The measurements were done using calibration curves prepared from mixtures of silica and Nb₂O₅ (Si/Nb from 5 to 300).

The N₂ adsorption/desorption isotherms at 77 K on materials under study were recorded using a static volumetric apparatus ASAP 2020 (Micromeritics). In order to attain a sufficient accuracy in the accumulation of the adsorption data, this instrument is equipped with pressure transducers covering the 133 Pa and 133 kPa ranges. Before each sorption measurement the samples were outgassed at 383–393 K overnight until the residual pressure was lower than 0.7 Pa. The surface area was calculated by the BET method, whereas the volume and the diameter of mesopores were estimated according to Broekhoff-de Boer method with the Frenkel–Halsey–Hill equation (BdB FHH).

Table 1 lists some characterization data of the catalysts under study.

UV-vis spectra were recorded using a Varian-Cary 300 Scan UV-visible Spectrophotometer. Sample powders were placed into the cell equipped with a quartz window. The spectra were recorded in the range from 800 to 190 nm. Spectral on (fluoropolymer standard provided with Varian Spectrometer) was used as a reference material.

Table 1

Alkali metal (Me) loading and textural parameters of NbMCF catalysts.

Sample	Me weightloading [%]	Me loading(mol/m ² g ⁻¹) * 10 ⁻⁶	Surface area, BET[m ² /g]	Mean pore volume [cm ³ /g] BdB FHH adsorption
NbMCF(ox)	–	–	672	2.7
Li/NbMCF(ox)	0.35	1.39	361	1.6
Na/NbMCF(ox)	1.15	1.69	296	1.3
K/NbMCF(ox)	1.96	2.02	248	1.2
Rb/NbMCF(ox)	4.27	2.21	226	1.2
Cs/NbMCF(ox)	6.67	1.99	231	1.1
NbMCF(Et)	–	–	717	2.8
Li/NbMCF(Et)	0.35	1.51	331	1.6
Na/NbMCF(Et)	1.15	1.47	341	1.5
K/NbMCF(Et)	1.96	1.65	303	1.7
Rb/NbMCF(Et)	4.27	2.00	250	1.3
Cs/NbMCF(Et)	6.67	2.14	234	1.4

Two test reactions were used to determine acid-base properties of catalysts. They were 2,5-hexanedione cyclisation and dehydration and 2-propanol decomposition.

A tubular, down-flow reactor was used in 2,5-hexanedione cyclisation reaction that was carried out at atmospheric pressure, using nitrogen as the carrier gas. In a typical experiment, the catalyst bed (0.05 g) was first activated for 2 h at 673 K under nitrogen flow (40 cm³ min⁻¹). Subsequently, 0.5 cm³ of 2,5-hexanedione was passed continuously over the catalyst at 623 K. The substrate was delivered with a pump system and vaporized before being passed through the catalyst with the flow of nitrogen carrier gas (40 cm³ min⁻¹). The reaction products were collected for 30 min downstream of the reactor in the cold trap (mixture of 2-propanol and liquid nitrogen) and analysed by gas chromatography (CHROM-5, Silicone SE-30/Chromosorb G column).

The 2-propanol conversion (dehydration and dehydrogenation) was performed, using a microcatalytic pulse reactor inserted between the sample inlet and the column of a CHROM-5 chromatograph. In a typical experiment, the catalyst bed (0.02 g) was first activated at 673 K for 2 h under helium flow (40 cm³ min⁻¹). The 2-propanol conversion was studied at 423, 473, 523 and 573 K using 3 mL pulses of alcohol under helium flow (40 cm³ min⁻¹). The reactant and the reaction products: propene, 2-propanone (acetone) and diisopropyl ether were analysed using CHROM-5 gas chromatograph on line with microreactor. The reaction mixture was separated on 2 m column filled with Carbowax 400 (80–100 mesh) at 338 K in helium flow (40 cm³ min⁻¹) and detected by TCD.

2.4. Catalytic performance

The reactions were performed in a liquid phase under atmospheric pressure in a multi-experiment work station StarFish (Radley's Discovery Technologies UK).

In a typical procedure, 2-hydroxybenzaldehyde (**2**) (2 mmol), and ethyl cyanoacetate (**3**) (4 mmol) were added to the 3-necked vessel of 10 mL of capacity, equipped with condenser and thermometer and magnetic stirred (0.8 cm). Subsequently, the catalyst (50 mg) was added and the reaction mixture was stirred (250 rpm) at room temperature, 298 K, during the appropriated reaction time shown in figures or tables. The samples were taken at different reaction times by diluting a small amount of the reaction mixture in dichloromethane (0.5 mL). Subsequently, the catalyst was filtered off and the solvent evaporated *in vacuo*.

Activation of the catalyst samples was carried out at 333 K overnight.

The reactions were followed by TLC chromatography performed on DC-Aulofolien/Kieselgel 60 F245 (Merck) using mixtures of CH₂Cl₂/EtOH in 98:2 as eluent.

The characterization of the reaction products was carried out by ¹H NMR. NMR spectra were recorded with a Bruker AVANCE DPX-

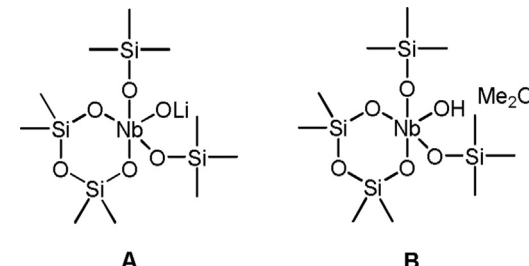


Chart 1. Structures selected as theoretical models for calculations.

300(300 MHz for ¹H). ¹H chemical shifts (δ) in CDCl₃ are given from internal tetramethylsilane.

All reagents and solvents were purchased from Aldrich, Fluka and Alfa-Aesar.

2.5. Theoretical calculations

The calculations were carried out with the Gaussian 09 suite of programs [22]. Geometry optimizations were performed using the B3LYP functional using the standard double-z quality plus polarization functions 6-31G(d,p) for all atoms but Nb and Cs, which were treated with the Los Alamos ECP [23]. Reactants and intermediates were characterized by frequency calculations, and have positive definite Hessian matrices. Transition-state structures (TS's) show only one negative eigenvalue in their diagonalized force-constant matrices, and their associated eigenvectors were confirmed to correspond to the motion along the reaction coordinate under consideration using the intrinsic reaction coordinate (IRC) method [24]. Vibrational frequencies were also performed to extract vibrational zero-point and thermal corrections from the thermodynamic results. Single-point calculations on the optimized geometries were performed with the dispersion-corrected M06 functional [25] with the expanded 6-311G(2d,p) basis sets to estimate more rigorous values.

In accordance with the basis of our accumulated observations on these materials, the selected models for the calculations are depicted in Chart 1.

3. Results and discussion

3.1. Nb loading and structure/textural characterization of MCF materials

The procedure of MCF synthesis originally proposed by Stucky et al. [21a] was modified in this work by the addition of niobium source at the end of the synthesis route [21c]. Two various TMB/PL ratios were applied (TMB/PL = 1.5 and 0.75) depending on

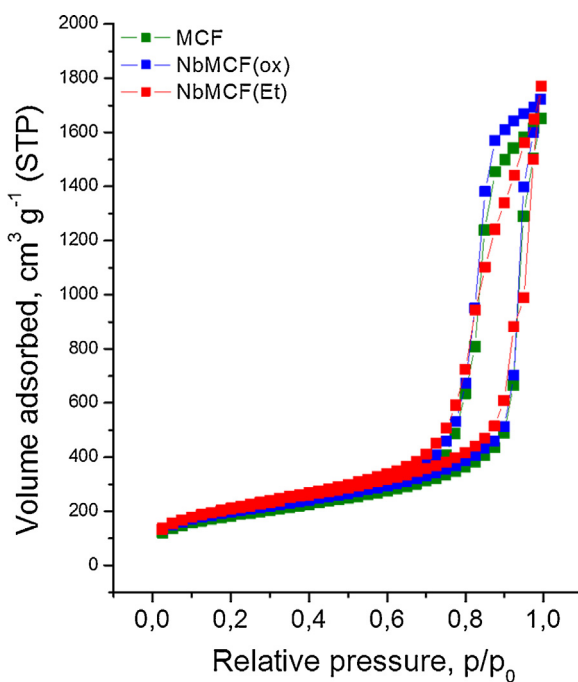


Fig. 1. Nitrogen adsorption isotherms of NbMCF supports.

the source of Nb used (ammonium niobate(V) oxalate hydrate or niobium ethoxide). In the case of NbMCF(Et), niobium ethoxide produces additional ethanol during the synthesis (this compound is also released during hydrolysis of TEOS). The higher concentration of ethanol enhances the transformation of cylindrical SBA-15 towards the spherical MCF phase. The lower TMB/PL ratio was used in this synthesis because the higher value of this ratio does not allow obtaining the proper material.

The loading of niobium in NbMCF materials was estimated on the basis of XRF data and it is lower than assumed (real Si/Nb ratio is 260 for NbMCF(ox) and 169 for NbMCF(Et)). The weight percent of Nb in NbMCF(ox) is significantly lower (0.5 ± 0.04 wt.%) than in NbMCF(Et) (0.8 ± 0.03 wt.%). It has been reported in the literature, that the introduction of niobium from Nb(V) oxalate under acid conditions in the synthesis typically gives materials with low niobium concentration [26].

The N_2 adsorption/desorption isotherms of MCF and NbMCF supports shown in Fig. 1 are typical of mesostructured cellular foams of MCF materials [28a] exhibiting a H1 type hysteresis loop at a relatively high pressure (p/p_0) with parallel adsorption and desorption branches for MCF and NbMCF(ox).

The nitrogen adsorption/desorption isotherm of NbMCF(Et) is slightly deformed in the desorption branch at the high p/p_0 ratio. The shape of isotherms does not change significantly for samples after modification with alkali metals with the exception of Cs/NbMCF(ox).

The texture parameters of NbMCF supports significantly change after their modification by impregnation with alkali metals (Table 1). The samples containing alkali metals exhibit much lower surface area than the unmodified ones. BET surface area is strongly dependent on the metal loading (expressed in $\text{mol}/\text{m}^2\text{g}^{-1}$ in Table 1) and it decreases with the growth of the alkali metal incorporated. Pore volume is changed in the same order. The nature of the alkali metal and the method of NbMCF preparation (ox or Et niobium source) are not crucial for the BET surface area value. As example for the role of metal loading, K/NbMCF(ox) (Me loading $2.02 \text{ mol}/\text{m}^2\text{g}^{-1}$) shows BET surface area $248 \text{ m}^2/\text{g}$ whereas Rb/NbMCF(Et) (Me loading $2.00 \text{ mol}/\text{m}^2\text{g}^{-1}$) exhibiting

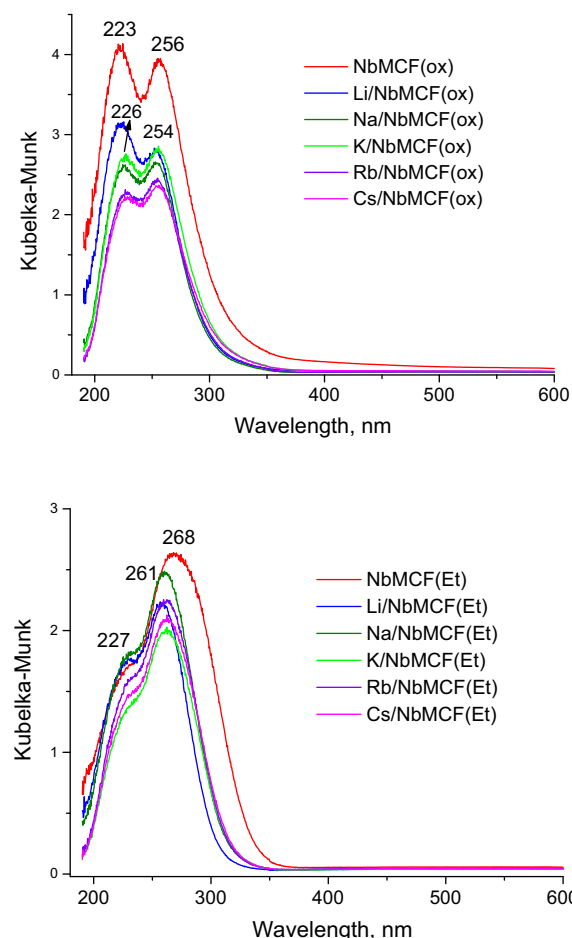


Fig. 2. UV-vis spectra of NbMCF catalysts before and after the modification with alkali metals.

surface area of $250 \text{ m}^2/\text{g}$. Textural parameters calculated from N_2 adsorption/desorption isotherms are shown in Table 1.

The morphology of NbMCF supports is illustrated by SEM images (Fig. S1—Supplementary data). All materials show a coral-type morphology characteristic of MCF materials.

3.2. Niobium state in MCF materials

The location of niobium introduced during the synthesis of MCF material (NbMCF) was explained by metal coordination studied using UV-vis technique. UV-vis spectra of both series of Nb-containing catalysts (Fig. 2A and B) show two UV bands at 223 and 256 nm for NbMCF(ox) and 227 and 268 nm for NbMCF(Et) from low coordinated (tetra and penta) niobium species localized in the framework of MCF [21c,27]. These two bands can be assigned to the electron charge transfer typical of niobium in the framework positions in different surroundings [21c]. This diversity of surroundings comes from the structure of MCF (windows and cells) and the possible non-uniform distribution of niobium. However, it is important to note, that the relative intensity of the UV-vis bands varies depending on the NbMCF series. The lack of the UV-vis bands at $\sim 330 \text{ nm}$ characteristic of octahedrally coordinated Nb proves the absence of extra framework niobium species on the surface of all samples studied. It is important to stress that the small variation in the position of the bands in UV-vis spectra of NbMCF materials after modification indicates the interaction of alkali metal species with niobium located in the supports.

The higher shift of the band position is noted for the series of catalysts based on NbMCF(Et). In this series the intensity of UV-vis band at 268 nm corresponding to the charge transfer in pentacoordinated oxo-niobium species is much higher than that at ca 227 nm coming from charge transfer in tetracoordinated niobium. It is not a case of NbMCF(ox) series where both UV-vis bands show almost the same intensity. It is a significant difference in the both series of catalysts. Recently calculations [28] have indicated that this pentacoordinated niobium species, being one of the most stable, is tetra-anchored to the silica structure and the fifth coordination is with hydroxyl group – potentially catalytic active centers. Anchoring of Nb-species via ethoxy groups present in Nb-source (Et) is much easier by interaction with silanol groups than via oxalate ligands in Nb-source(ox). Therefore, in the case of NbMCF(Et) tetra-anchored pentacoordinated niobium species dominate.

3.3. Acid-base properties of catalysts—test reactions

The presence of Nb in mesoporous structure of MCF influences the basic properties of the alkali modified samples. Two types of reactions have been tested in this work to study the acidity/basicity of the surface of the catalysts prepared: 2-propanol decomposition and 2,5-hexanedione cyclisation and dehydration.

3.3.1. Propanol (2-PrOH) decomposition

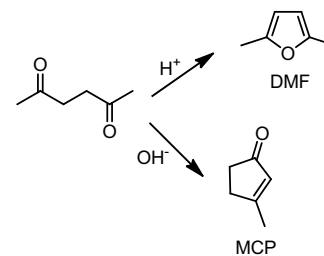
The 2-propanol decomposition is a test reaction for characterisation of acidic (Brønsted or Lewis) and/or basic properties of solids [29]. Dehydration of alcohol to propene and/or diisopropyl ether requires acidic centers (Lewis or Brønsted), whereas the dehydrogenation to acetone occurs on Lewis basic sites.

As shown in Table 2, over both Nb-containing matrices (NbMCF(ox), NbMCF(Et)) the main reaction product of 2-propanol decomposition, at 523 and 573 K, is propene, so these results indicate the acidic character of these supports. The activity of MCF is below 1% of 2-propanol conversion. The activity of MCF increases when Nb is introduced to the MCF framework (Table 2) and depends on the preparation procedure (ox or Et used as Nb source). It is clear that more niobium species (Lewis acid sites) incorporated from ethoxide give rise to the higher acidic activity in 2-propanol reaction. Moreover, one can suppose that hydroxyls present in pentacoordinated niobium species are also responsible for this activity. Interestingly, NbMCF(ox) shows not only dehydration but also dehydrogenation activity indicating that this support contains also Lewis basic sites responsible for transformation of 2-propanol to acetone.

The impregnation of acidic NbMCF supports with alkali metal acetates decreases the activity of the catalyst towards 2-PrOH dehydration/dehydrogenation below 1% of conversion. As a result of the poisoning of the supports acidic centers by alkali metals, the catalysts based on niobiosilicates are not active. Therefore the results of 2-propanol decomposition on alkali modified materials are not considered in the discussion.

3.3.2. 2,5-Hexanedione cyclisation and dehydration

The cyclisation and dehydration of 2,5-hexanedione has been used as a test reaction for Brønsted basicity/acidity properties of the catalysts [30]. The formation of 2,5-dimethylfuran (DMF) occurs on acidic centers, whereas in the production of 3-methyl-2-cyclopentenone (MCP) basic centers take part (Scheme 2). On the basis of the ratio of selectivity to MCP/selectivity to DMF, the sequence of the basicity of the prepared catalysts can be estimated. According to the literature [30,31] the basicity of the catalyst is stated if $MCP/DMF \gg 1$. When $MCP/DMF \ll 1$ the catalyst exhibits acidic properties, while for $MCP/DMF \sim 1$ the acid–base character of catalysts is postulated.



Scheme 2. 2,5-Hexanedione transformation in acid and in basic medium.

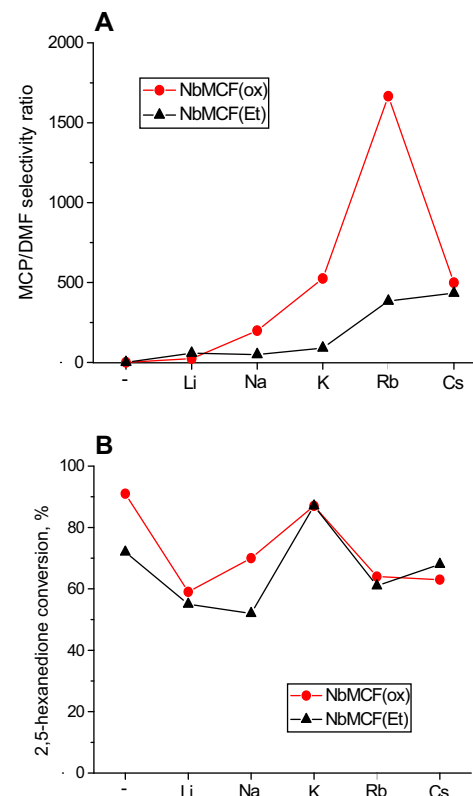


Fig. 3. (A) Dependence of the MCP/DMF selectivity ratio on the nature alkali metals located on the surface of NbMCF(ox) and NbMCF(Et); (B) conversion of 2,5-hexanedione.

The conversion of 2,5-hexanedione and selectivity ratio MCP/DMF are shown in Fig. 3. The conversion of 2,5-hexanedione depends strongly on the composition of the matrix. The activity is higher for NbMCF(ox) than NbMCF(Et). The sequence of conversion for NbMCF supports differs from that of 2-propanol reaction. However, one should remember that the mechanisms of both processes are different. In 2-propanol conversion a large variety of reaction pathways is possible involving both types of acid (Brønsted and Lewis) and Lewis base centers. In 2,5-hexanedione cyclisation Brønsted acid and/or base centers are required.

NbMCF(Et) and NbMCF(ox) materials exhibit acidic properties ($MCP/DMF \gg 1$).

The effect of the alkali metal on the activity and selectivity of catalysts is clearly visible. The decrease of activity of NbMCF supported materials is observed. It indicates that impregnation procedure blocks most of the Brønsted acid centers present on the surfaces of NbMCF(ox) and NbMCF(Et). The introduction of alkali metals generates Brønsted basic centers—the selectivity to MCF significantly increases for all modified catalysts studied. It can be observed a volcanic dependence of MCP/DMF selectivity ratio vs the nature of alkali metal element for NbMCF(ox) supported catalysts (Fig. 3A),

Table 2

The results of 2-propanol decomposition.

Catalyst	Temperature [K]	2-PrOH conv. [%]	Propene sel. [%]	Acetone sel. [%]
MCF	523	<1	100	—
	573	<1	100	—
NbMCF(ox)	523	1	85	15
	573	7	97	3
NbMCF(Et)	523	18	100	—
	573	59	100	—

on which the highest MCP/DMF ratio was noted for sample containing rubidium. It is not the case of NbMCF(Et) series. For this type of catalysts the MCP/DMF ratio systematically increases from Li to Cs modified material. Moreover, NbMCF(Et) based catalysts are characterized by the lowest Brønsted basicity. However, it is important to stress that for both series of catalysts the highest activity in the cyclisation and dehydration of 2,5-hexanedione is noted for samples modified with potassium (Fig. 3B). Taking into account the MCP/DMF ratio for potassium modified matrices, the following order is observed: K/NbMCF(ox) > K/NbMCF(Et). The higher acidic activity of the support the lower basic activity of potassium containing catalysts is achieved.

3.4. Catalytic performance

MCF catalysts were tested in the reaction of 2-hydroxybenzaldehyde (**2a**) and ethyl cyanoacetate (**3**), at room temperature, under solvent-free conditions (Scheme 3). Firstly, we carried out the reaction in the presence of MCF and both NbMCF supports (ox and Et series). It should be noted that only in the presence of NbMCF(ox) a mixture chromenes **4a** and **5a** were obtained in almost 5% of yield after 4 h of reaction time. These preliminary results suggest that the environment provided by hydroxyl groups and Nb present in the investigated supports, exhibiting very different acid-base properties, are not probably involved in the reaction or they are barely able to activate the first step of the reaction, that is, the aldolic condensation between reagents. Remarkably, the blank experiment under the same experimental conditions did not produce any reaction product recovering the unaltered starting reagents.

The modification of the NbMCF supports with alkaline metals yielded, in all the investigated cases, diastereomeric mixtures (*Erythro/Threo* isomers) of the chromenes **4a** and **5a**. Fig. 4 shows the yield of chromenes **4a** and **5a** in the reaction catalyzed by Me/NbMCF materials, after 60 min (Fig. 4A) and 120 min of reaction times (Fig. 4B). It can be observed a different catalytic behavior for the modified NbMCF materials as function of the used NbMCF support, as expected. The yield of chromenes **4a** and **5a** in the presence of Me/NbMCF(Et) decreases when the cation size of the alkaline metal is increased. Similar trend was observed when using the NbMCF(ox) series, Li/NbMCF being an exception. It is important to note that the best yields of compounds **4a** and **5a** were obtained when the reaction was catalyzed by Na or K/NbMCF(ox) after 60 min of reaction time (Fig. 4A), although similar conversion were observed when the reaction was carried out in the presence of Li/NbMCF(Et) after 120 min.

These results were rationalized in terms of metal loading on the corresponding NbMCF series but also regarding the acid-base properties of the corresponding catalysts. Concerning to the alkaline metal content, Na or K/NbMCF(ox) showed higher metal loading (expressed in mol/m²g⁻¹ × 10⁻⁶, Table 1) as compared with their Et series homologues. This fact is also demonstrated for the Li/NbMCF(Et) catalyst. In other sense, it is clear the influence of the alkaline metal in the reaction since other Me/NbMCF(ox or Et) with higher metal loadings afforded mixtures of compounds **4a** and **5a** with lower yields (Table 1 and Fig. 4).

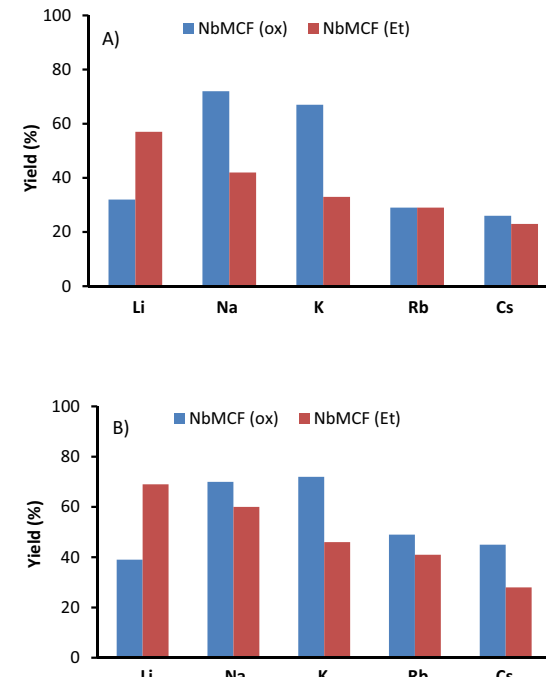
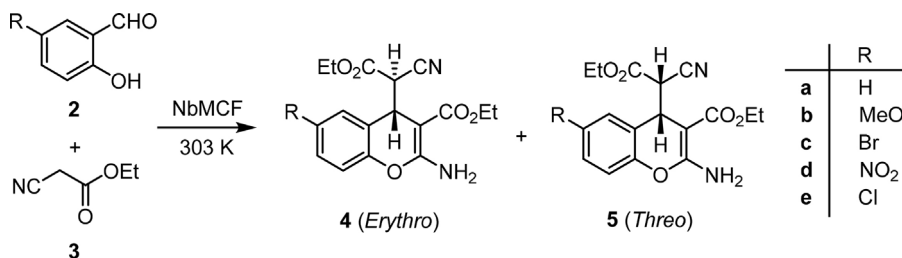
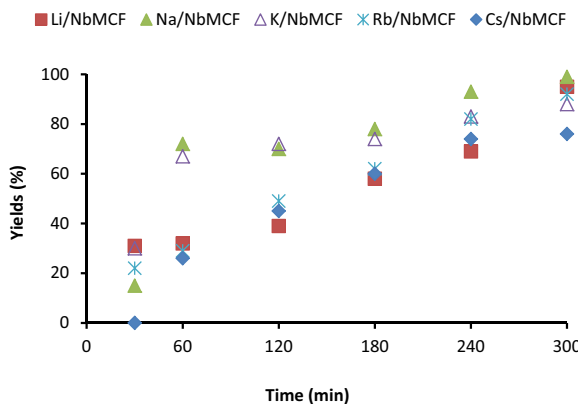
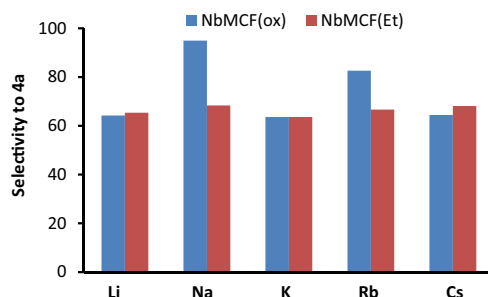


Fig. 4. Yields of chromenes **4a** and **5a** from 2-hydroxybenzaldehyde (**2a**) and ethyl cyanoacetate (**3**), at room temperature, under solvent-free conditions, catalyzed by Me/NbMCF materials, (A) after 60 min and (B) after 120 min of reaction times.

The results seem to indicate that the Brønsted basic centers created by the modification of NbMCF(ox) with alkaline metals could be the responsible of the observed reactivity. Also, the reaction is catalyzed by Lewis basic centers, although in lower extent. This circumstance is likewise demonstrated by the observed lower catalytic activity for the NbMCF(ox) support and Me/NbMCF(Et), the Et series characterized by exhibiting lower Brønsted basicity.

The yields of compounds **4a** and **5a**, at different reaction times, when the reaction is catalyzed by Me/NbMCF(ox) are shown in Fig. 5. As can be observed, the best conversion values were obtained in the presence of Na or K/NbMCF(ox) affording mixtures of compounds **4a** and **5a** with almost quantitative yields after 5 h of reaction time. The major difference with their Me/NbMCF analogues is at shorter reaction times. Taken into account that Rb/NbMCF(ox) was the most basic catalyst, it then seems that the optimum Brønsted basicity is required to obtain the highest conversion values to chromenes **4a** and **5a** and it is provided by modification of NbMCF(ox) with Na or K acetates.

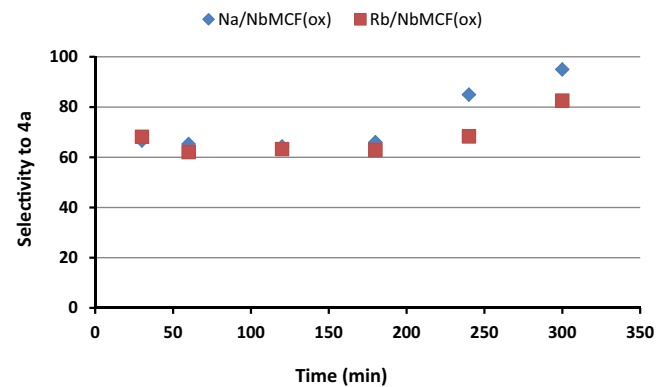
Having these results in mind, it seems reasonable to compare the catalytic behavior of the most efficient catalysts, Me/NbMCF (where Me is Na or K) with the analogues alkali metal oxides supported over MCF pure silica. The reaction under the same experimental conditions, in the presence of Na/MCF or K/MCF, yielded mixtures of chromenes **4a/5a** in 58 and 47%, after 1 h of reaction time, respectively; these yields are considerably lower than that obtained for

**Scheme 3.** Synthesis of 2-amino-4H-chromenes (**4** and **5**) from 2-hydroxybenzaldehyde (**2a**) and ethyl cyanoacetate (**3**).**Fig. 5.** Plot of yields of mixtures of chromenes **4a** and **5a** vs time, for the reaction between 2-hydroxybenzaldehyde (**2a**) and ethyl cyanoacetate (**3**), at room temperature, under solvent-free conditions, catalyzed by Me/NbMCF(ox) materials.**Fig. 6.** Selectivity to chromene **4a**, for the reaction between 2-hydroxybenzaldehyde (**2a**) and ethyl cyanoacetate (**3**), at room temperature, under solvent-free conditions, catalyzed by Me/NbMCF materials, after 300 min of reaction time.

Me/NbMCF. Therefore, Nb in the Me/NbMCF should be probably involved in the reaction favoring the process.

In general, chromenes **4a** and **5a** were obtained in approximately 2:1 ratio, the regioselectivity remaining constant along the reaction course. However, selectivity to compound **4a**, the most stable diastereomer, was notably increased when using Na and Rb/NbMCF(ox), 95 and 88, respectively (Fig. 6). Firstly, it could be due to the confinement effects derived from the smallest pore volume of these materials, 1.3 and 1.2 cm³/g, respectively. In Fig. 7 it is shown the variation of selectivity to chromene **4a** when using Na and Rb/NbMCF(ox) catalysts. As can be observed, the selectivity remains constant at the shortest reaction times as expected. However, an increase of the selectivity to **4a** is produced at the highest reaction times. These results indicate that in the presence of these catalysts, another competitive reaction, consisting of the epimerization reaction of the isomer **5a** into **4a**, is probably produced.

We also performed the reaction in the presence of small amount (25 mg) of the best catalytic material, Na/NbMCF(ox), yielding a mixture of chromenes **4a** and **5a** with lower conversion (66% after

**Fig. 7.** Variation of selectivity to **4a** vs time for the reaction between 2-hydroxybenzaldehyde (**2a**) and ethyl cyanoacetate (**3**), at room temperature, under solvent-free conditions, catalyzed by Me/NbMCF materials (where Me is Na or Rb).**Table 3**

Synthesis of chromenes **4** and **5** from differently substituted 2-hydroxybenzaldehydes (**2**) and ethyl cyanoacetate (**3**) catalyzed by Na/NbMCF.

R	Time (min)	Yield (%) ^a	Selectivity to 4
H	240	93 (72)	65
MeO	300	87 (44)	64
Br	300	72 (41)	71
NO ₂	240	95 (19)	75
Cl	60	82	70

^a Conversion values in parenthesis after 60 min of reaction time.

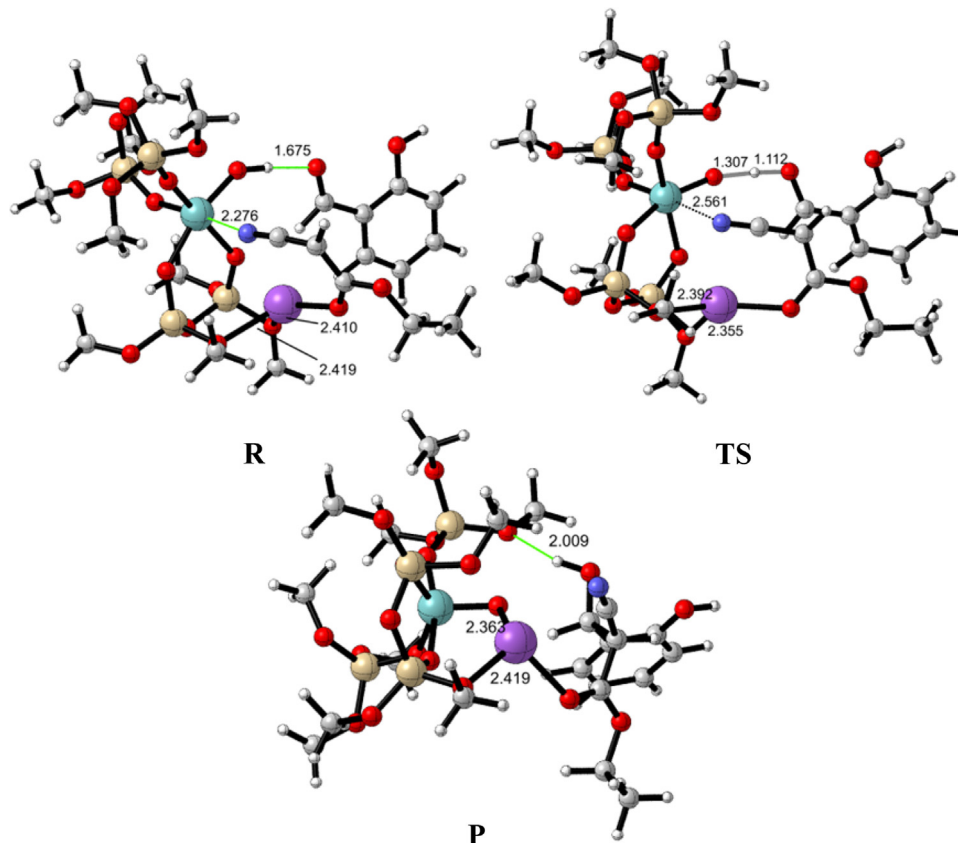
5 h of reaction time) and also decreasing the estereoselectivity to compound **4a**.

The scope of the methodology was investigated by starting from differently 5-substituted-2-hydroxybenzaldehydes (**2**) in the presence of one of the most active catalyst, Na/MCF(ox) (Table 3). In this sense, cromenes **4** and **5** were efficiently synthetized with good to excellent yields. The reactivity order of 5-substituted-2-hydroxybenzaldehydes **2** was Cl > H > MeO, Br > NO₂. Taken into account the experimental results, it can be concluded that the substitution at position 5– has a negative effect on the yield values obtained after 60 min of reaction times. However, the presence of the Cl atom at position 5– produces a notable increasing of conversion values to products **4** and **5**. In general, the presence of electro-withdrawing substituents at position 5– induces a slightly increasing of the selectivity to the major isomer **4** due probably to confinement effects.

Finally, the Table 4 summarizes the experimental conditions and results as comparison of the performance of the catalyst Na/NbMCF with respect to the previous literature. We report herein a new methodology for the synthesis of chromenes which uses the lowest catalyst amount, in absence of any solvent, operating at room temperature, during relatively short reaction times affording mixtures of chromenes **4** and **5** with good to excellent yields.

Table 4Heterogeneous catalysts involved in the synthesis of chromenes **4** and **5**.

Catalyst	HB/ECA	Catalyst amount (g)	Solvent	T (°C)	Time (h)	Yield (%)	.
Amberlyst-21	Substituted 2-hydroxybenzaldehydes 5/10 2-hydroxybenzaldehyde 5/10	2 2	EtOH EtOH	r.t. r.t.	2–5 4	68–94 85	[18]
SnMgAl-1	Substituted 2-hydroxybenzaldehydes 1/2 2-Hydroxybenzaldehyde 1/2	0.05 0.05	– –	40 °C 40 °C	1–24 18 (1)	83–94 98 (94)	[19]
MgAl	Substituted 2-hydroxybenzaldehydes 1/2 2-Hydroxybenzaldehyde 1/2	0.05 0.05	– –	40 °C 40 °C	20–24 24	83–98 88	[19]
Molecular sieve 3A	Substituted 2-hydroxybenzaldehydes 10/22	3	EtOH	r.t.	14	46–86	[20]
Molecular sieve 4A	5-Bromo-2-hydroxybenzaldehyde 10/22	3	EtOH	r.t.	14	56	[20]
Molecular sieve 5A		3	EtOH	r.t.	14	50	[20]
Al ₂ O ₃		3	EtOH	r.t.	14	63	[20]
Na/NbMCF	Substituted 2-hydroxybenzaldehydes 2/4 2-Hydroxybenzaldehyde 2/4	0.05 0.05	– –	r.t. r.t.	1–4 1	72–95 70	This work This work

**Fig. 8.** Optimized structures for the aldolization step catalyzed by Na/NbMCF.

HB/ECA: 2-hydroxybenzaldehydes (mmol)/ethyl cyanoacetate (mmol).

3.5. Computational study

Initially, we considered the model A in our calculations (Chart 1). Thus, it could be envisaged that the alkaline center could activate the ethyl cyanocetate **3** to form the C–C bond with salicylaldehyde **2a**. However, the postulated reaction mode did not lead to a productive reaction, in part due to the lack of a proper stabilization of the negative charge developed in the aldolic intermediate.

On other hand, if we assume the model B, we can propose that the basicity of the alkaline oxide is strong enough to easily activate the ethyl cyanocetate **3**, by abstraction of the methylenic proton, to form the reactive enolate. Under these conditions, the hydroxyl group of the catalyst can act as a Brønsted acid site, thus stabilizing the forming aldol transition structure. In addition, the Nb center

could promote the approaching of the reactants by interaction with the cyanocetate.

Our calculations reveal that the activation of the ethyl cyanocetate **3** by the alkaline oxide is a highly exothermic step and proceeds without activation barrier, as expected from such strong bases. The computed free energies of this activation are –39.5, –82.5 and –94.3 kcal/mol for Li, Na and Cs, respectively.

Once the nucleophile has been activated, the interaction with the Nb supported structure leads to the reactant complex **R** (Fig. 8), where the hydroxyl substituent forms a strong hydrogen-bond with the aldehyde carbonyl (1.661, 1.675 and 1.723 Å, for Li, Na and Cs). Moreover, the alkaline center interacts with two methoxy moieties of the silica support, and the Nb interacts with the cyano group (2.275, 2.276 and 2.286 Å, for Li, Na and Cs). These interactions promote the reactants approaching to generate the aldol intermediate. It should be noted that this reactant complex, **R**, is more stable than the isolated reactants for the reaction involving Li

and Na (−16.9 and −7.8 kcal/mol, respectively) while the presence of Cs leads to a less stable complex (5.2 kcal/mol above the isolated reactants), likely due to its bulkiness.

The formation of the C–C bond in the transition state, **TS**, is more advanced in the presence of Cs, as suggest the forming C–C (Li: 2.172, Na: 2.179, Cs: 2.138 Å) whereas the O–H bond distance follows the opposite trend (Li: 1.085, Na: 1.112, Cs: 1.171 Å) which indicates a more asynchronous structure for the smaller alkaline metals. The activation barrier to reach the transition structure follows the order Cs (10.5) < Na (12.2) < Li (15.6 kcal/mol).

TS leads to the aldol intermediate, **I**, displaying the full formation of the C–C and O–H bonds. This structure shows notable differences depending of the alkaline center. Thus, the interaction between the Li and the methoxy moieties, on one hand, and the aldolic hydroxyl with the new sp^2 oxygen of the support, on the other hand, drives to a less stable complex than the reactant species **R** (by 3.4 kcal/mol). Conversely, for the aldolization involving Na and Cs centers, the aldolic hydroxyl moiety is displaced by the alkaline which thus interacts with the support deprotonated oxygen. In these cases, the reaction step is exothermic, being **I** more stable than the reactant complex **R** (−5.4 and −11.3 kcal/mol, for Na and Cs, respectively).

In summary, the strong basicity of the alkaline oxides activates the formation of the nucleophile. These results agree with the experimental observations since they revealed that the reaction is probably promoted by Brønsted basic sites and the reactivity is increased in the presence of the alkaline oxides. However, the bulkiness of the alkaline center has a deep impact on the formation and stability of the reactant complex, which is obstructed in the presence of the bulkier centers thus restricting the effective aldolization, in agreement with the reactivity found in the presence of the most basic materials.

4. Conclusions

We report herein an efficient and eco-friendly methodology for the synthesis of 2-amino-4H-chromenes from 2-hydroxybenzaldehyde **2** and ethyl cyanoacetate **3**, catalyzed by Me/NbMCF. The reaction takes place under solvent-free conditions, at room temperature, leading to mixtures of the corresponding chromenes **4** and **5**, in a 2:1 ratio, with good to excellent yields, in all the cases the *erythro* isomer being the major compound.

The different Nb sources for the preparation of the investigated catalysts and the subsequent modification with the corresponding alkaline metals acetates provide them different textural and acid-base characteristics. Considering that, the reaction is probably promoted by Brønsted basic sites over the catalyst, Na or K/NbMCF being the most efficient materials, although the activation by the Lewis basic centers cannot be neglected.

Our experimental observations suggest that the alkaline metals and Nb are involved in the reaction. Although NbMCF supports were not active for the synthesis of chromenes, it seems that Nb and alkaline metals could act in cooperation favoring the process. The metal loading on the catalysts under study but also the acid-base character and probably the texture properties are the key parameters controlling the reaction and diastereoselectivity. When the reaction is catalyzed by the most efficient catalyst (Na/NbMCF(ox)) or the most basic one (Rb/NbMCF(ox)), the selectivity of the reaction is altered probably by producing a competitive epimerization reaction of chromene **5a** to **4a**.

The computational study suggests that the strong basicity of alkaline oxides initiates the reaction by activation of the reactants. However, the formation of the reactant complex and effective reaction requires a compromise between this basicity and the alkaline center size.

Acknowledgements

This work has been supported in part by MICINN (projects and CTQ2011-27935 and CTM2014-56668-R) and National Science Centre in Poland (Project No. 2014/15/B/ST5/00167). We are grateful to the Centro de Supercomputación de Galicia (CESGA) for generous allocation of computing resources.

Appendix A. Supplementary data

Supplementary data associated with this article can be found, in the online version, at <http://dx.doi.org/10.1016/j.cattod.2016.02.042>.

References

- [1] J.S. Beck, J.C. Vartuli, W.J. Roth, M.E. Leonowicz, C.T. Kresge, K.D. Schmitt, C.T.W. Chu, D.H. Olson, E.W. Sheppard, S.B. McCullen, J.B. Higgins, J.L. Schlenker, *J. Am. Chem. Soc.* 114 (1992) 10834–110834.
- [2] C. Martínez, A. Corma, *Coord. Chem. Rev.* 255 (2011) 1558–1580.
- [3] L.T. Burness, *Mesoporous materials: properties, in: Preparation and Applications*, Nova Science Publishers, New York, 2007.
- [4] T. Yokoia, Y. Kubotab, T. Tatsumia, *Appl. Catal. A: Gen.* 421–422 (2012) 14–37.
- [5] S. Loganathan, M. Tikmani, A.K. Ghoshal, *Langmuir* 29 (2013) 3491–3499.
- [6] (a) A. Olea, E.S. Sanz-Pérez, A. Arencibia, R. Sanz, G. Calleja, *Adsorption* 19 (2013) 589–600;
 (b) N. Hiyoshi, K. Yogo, T. Yashima, *Microporous Mesoporous Mater.* 84 (2005) 357–365;
 (c) N. Hiyoshi, K. Yogo, T. Yashima, *Chem. Lett.* 33 (2004) 510–511.
- [7] X. Feng, G. Hu, X. Xu, G. Xie, Y. Xie, J. Lu, M. Luo, *Ind. Eng. Chem. Res.* 52 (2013) 4221–4228.
- [8] B. Dragoi, E. Dumitriu, C. Guimon, A. Auroux, *Micropor. Mesopor. Mater.* 121 (2009) 7–17.
- [9] J. Zhu, T. Wang, X. Xu, P. Xiao, J. Li, *Appl. Catal. B: Env.* 130–131 (2013) 197–217.
- [10] (a) E. Pérez-Mayoral, V. Calvino-Casilda, M. Godino, A.J. López-Peinado, R.M. Martín-Aranda, *Porous catalytic systems in the synthesis of bioactive heterocycles and related compounds, in: G. Brahmachari (Ed.), Biologically Relevant Heterocycles*, Elsevier, 2015, pp. 378–403;
 (b) E. Pérez-Mayoral, E. Soriano, R.M. Martín-Aranda, F.J. Maldonado-Hódar, *In: Mesoporous Catalytic Materials and Fine Chemistry, in: M. Aliofkharrae (Ed.), Comprehensive Guide for Mesoporous Materials. Volume 1: Synthesis and Characterization*, Nova Science Publishers, Inc., 2015, Series: Materials Science and Technologies.
- [11] (a) A. Smuszkiewicz, E. Pérez-Mayoral, E. Soriano, I. Sobczak, M. Ziolek, R.M. Martín-Aranda, A.J. López-Peinado, *Catal. Today* 218–219 (2013) 70–75;
 (b) A. Smuszkiewicz, J. López-Sanz, E. Pérez-Mayoral, E. Soriano, I. Sobczak, M. Ziolek, R.M. Martín-Aranda, A.J. López-Peinado, *J. Mol. Catal. A: Chem.* 378 (2013) 38–46.
- [12] P. Schmidt-Winkel, W.W. Lukens Jr., Peidong Yang, D.I. Margolese, J.S. Lettow, J.Y. Ying, G.D. Stucky, *Chem. Mater.* 12 (2000) 686–696.
- [13] K. Stawicka, M. Trejda, M. Ziolek, *Appl. Catal. A: Gen.* 467 (2013) 325–334.
- [14] (a) K. Stawicka, M. Trejda, M. Ziolek, *Microporous Mesoporous Mater.* 181 (2013) 88–98;
 (b) M. Trejda, K. Stawicka, M. Ziolek, *Catal. Today* 192 (2012) 130–135.
- [15] I. Sobczak, M. Kołowska, M. Ziolek, *J. Mol. Catal. A: Chem.* 390 (2014) 114–124.
- [16] C. Bingi, N.R. Emmadi, M. Chennapuram, Y. Poornachandra, C. Ganesh Kumar, J. Babu Nanobulu, K. Atmakur, *Bioorg. Med. Chem. Lett.* 25 (2015) 1915–1919.
- [17] H.G. Kathroliya, M.P. Patel, *Med. Chem. Res.* 21 (2012) 3406–3416.
- [18] J.S. Yadav, B.V. Subba Reddy, M.K. Gupta, I. Prathap, S.K. Pandey, *Catal. Commun.* 8 (2007) 2208–2211.
- [19] U. Costantino, M. Curini, F. Montanari, M. Nocchetti, O. Rosati, *Microporous Mesoporous Mater.* 107 (2008) 16–22.
- [20] N. Yu, J.M. Aramini, M.W. Germann, Z. Huang, *Tetrahedron Lett.* 41 (2000) 6993–6996.
- [21] (a) D. Zhao, J. Feng, Q. Huo, N. Melosh, G.H. Fredrickson, B.F. Chmelka, G.D. Stucky, *Science* 279 (1998) 548–552;
 (b) J.S. Lettow, Y.J. Han, P. Schmidt-Winkel, P. Yang, D. Zhao, G.D. Stucky, J.Y. Ying, *Langmuir* 16 (2000) 8291–8295;
 (c) K. Stawicka, I. Sobczak, M. Trejda, B. Sulikowski, M. Ziolek, *Microporous Mesoporous Mater.* 155 (2012) 143–152.
- [22] M.J. Frisch, G.W. Trucks, H.B. Schlegel, G.E. Scuseria, M.A. Robb, J.R. Cheeseman, G. Scalmani, V. Barone, B. Mennucci, G.A. Petersson, H. Nakatsuji, M. Caricato, X. Li, H.P. Hratchian, A.F. Izmaylov, J. Bloino, G. Zheng, J.L. Sonnenberg, M. Hada, M. Ehara, K. Toyota, R. Fukuda, J. Hasegawa, M. Ishida, T. Nakajima, Y. Honda, O. Kitao, H. Nakai, T. Vreven, J.A. Montgomery, J.E. Peralta Jr., F. Ogliaro, M. Bearpark, J.J. Heyd, E. Brothers, K.N. Kudin, V.N. Staroverov, T. Keith, R. Kobayashi, J. Normand, K. Raghavachari, A. Rendell, J.C. Burant, S.S. Iyengar, J. Tomasi, M. Cossi, N. Rega, J.M. Millam, M. Klene, J.E. Knox, J.B. Cross, V. Bakken, C. Adamo, J. Jaramillo, R. Gomperts, R.E. Stratmann,

- O. Yazyev, A.J. Austin, R. Cammi, C. Pomelli, J.W. Ochterski, R.L. Martin, K. Morokuma, V.G. Zakrzewski, G.A. Voth, P. Salvador, J.J. Dannenberg, S. Dapprich, A.D. Daniels, O. Farkas, J.B. Foresman, J.V. Ortiz, J. Cioslowski, D.J. Fox, Gaussian 09 Revision B.01, Gaussian Inc, Wallingford, CT, 2010.
- [23] W.R. Wadt, P.J. Hay, *J. Chem. Phys.* 82 (1985) 284–298.
- [24] C. González, H.B. Schlegel, *J. Phys. Chem.* 94 (1990) 5523–5527.
- [25] Y. Zhao, D.G. Truhlar, *Acc. Chem. Res.* 41 (2008) 157–167.
- [26] B. Kilos, A. Tuel, M. Ziolek, J.-C. Volta, *Catal. Today* 118 (2006) 416–424.
- [27] M. Nashimura, K. Asakura, Y. Iwasawa, *J. Chem. J. Chem. Soc. Chem. Commun.* 15 (1986) 1660–1661.
- [28] D.C. Tranca, A. Wojtaszek-Gurdak, M. Ziolek, F. Tielens, *PCCP* 17 (2015) 22402–22411.
- [29] A. Gervasini, J. Fenyvesi, A. Auroux, *Catal. Lett.* 43 (1997) 219–228.
- [30] R.M. Dessau, *Zeolites* 10 (1990) 205–206.
- [31] J.J. Alcaraz, B.J. Arena, R.D. Gillespie, J.S. Holmgren, *Catal. Today* 43 (1998) 89–99.